PHYSICAL REVIEW B, VOLUME 63, 060501(R)

Vortex pinning by magnetic order in $ErNi_2B_2C$

C. D. Dewhurst,[1,*] S. S. James,[2] R. A. Doyle,[2,†] Y. Paltiel,[3] H. Shtrikman,[3] E. Zeldov,[3] and D. McK. Paul[1]

[1]*Department of Physics, University of Warwick, Coventry CV4 7AL, United Kingdom*

[2]*Interdisciplinary Research Centre in Superconductivity, University of Cambridge, Cambridge CB3 OHE, United Kingdom*

[3]*Department of Condensed Matter Physics, The Weizmann Institute of Science, 76100 Rehovot, Israel*

(Received 6 March 2000; published 29 December 2000)

We have used a miniature linear Hall probe array to make local magnetization measurements of the magnetic superconductor $ErNi_2B_2C$ ($T_c \simeq 10.8$ K). We show the sharp onset of significant pinning effects in $ErNi_2B_2C$ is coincident with the onset of an *a*-axis incommensurate ordering of the Er moments at $T_a^m \simeq 6$ K, below T_c. The data presented provide further evidence that certain components of the magnetic order in $(R)Ni_2B_2C$ materials interact with the vortex lattice and have a profound influence on the nonequilibrium (vortex pinning) properties of the superconducting state.

DOI: 10.1103/PhysRevB.63.060501 PACS number(s): 74.25.Ha, 74.25.Dw, 74.60.−w, 74.70.Ad

The rare-earth nickel borocarbides $[(R)Ni_2B_2C]$ are an interesting class of materials which can exhibit both superconductivity and magnetic order at low temperatures. For a review see Refs. 1 and 2. The superconducting transition temperature, T_c, varies from about 15 K for $R=$ Y and Lu to 6 K for Dy, with the Ginzburg-Landau parameter $\kappa > 5$ and upper critical fields, B_{c2}, as high as 10 T. Antiferromagnetic order in the $(R)Ni_2B_2C$ materials is not simple and is incommensurate in most cases.[1–5] $ErNi_2B_2C$ orders magnetically at $T_a^m \simeq 6$ K into an incommensurate transversely polarized spin-density wave along the *a* axis with wave vector (0.5526,0,0),[1,3] and coexists with weak ferromagnetic order below $\simeq 2.5$ K.[6] $HoNi_2B_2C$ exhibits commensurate antiferromagnetism below $\simeq 5$ K and incommensurate order described by two modulation vectors (0.59,0,0) and (0,0,0.92) between 5 K$<T<$6 K and 5 K$<T<\simeq$8 K, respectively.[1,4,5] The onset of *a*-axis incommensurate order in both materials is thought to be responsible for strong pair breaking and the suppression of B_{c2} close to the ordering temperature.[4,5]

Small angle neutron-scattering (SANS) measurements of the mixed state[7–10] show several field-dependent alignments of the vortex lattice to particular crystallographic directions implying a direct coupling of vortices to the underlying crystal symmetry. A coupling of vortices to the magnetic order in $ErNi_2B_2C$ has been inferred from SANS measurements which show a rotation of vortices away from the applied field direction and disordering due to increased pinning in the weakly ferromagnetic state below $\simeq 2.5$ K.[7] Recently, we have reported vortex pinning studies of $HoNi_2B_2C$ using miniature local Hall probes.[11] There we have shown that significant flux pinning in $HoNi_2B_2C$ becomes active between 5 and 6 K only, coincident with the appearance of the *a*-axis incommensurate order. We have argued that these two observations might be related and that the *a*-axis incommensurate magnetic phase may introduce pinning effects for vortices. In this paper we show that the vortex lattice in $ErNi_2B_2C$ is also weakly pinned and dominated by geometrical[12–14] and surface barriers[13,15] over much of the phase diagram. Bulk pinning only becomes significant below about 6 K and, in an analogous manner to $HoNi_2B_2C$,[11] is strongly correlated with the development of an *a*-axis incommensurate ordering of the Er moments.

Single crystals of $ErNi_2B_2C$ were grown using a high-temperature flux method.[2] Regular shaped crystals were separated from the Ni_2B flux and precharacterized using global magnetization (VSM) and resistivity measurements to confirm a sharp superconducting transition at $T_c \simeq 10.8$ K and antiferromagnetic transition at $T_a^m \simeq 5.8$ K. Crystals were cut into bars of dimensions around 1.2 mm$\times$170 μm and thicknesses around 60 μm using a miniature wire saw. One of the optically smooth, as-prepared, surfaces of the crystal ($\perp c$) was positioned directly onto the GaAs / AlGaAs Hall array[13] of 11 sensors of active area 10$\times$10 μm and spacing 10 μm [Fig. 1(b) inset].

Figure 1 shows local magnetization curves, $B_z - B_1$ vs edge field, B_1, and field profiles for a single crystal of $ErNi_2B_2C$ at 7.2 K. The data presented are representative of those measured at high temperatures above the magnetic ordering temperature, T_a^m and close to T_c. Figure 1(a) shows magnetization curves as determined by sensors 3, 6, and 9 located at the left edge, center, and right edge of the crystal, respectively. Flux penetration appears to occur first at the sample center (B_{p6}) and only later at the sample edges (B_{p3} and B_{p9}). Hysteresis is widest for the magnetization recorded at the sample edges, opposite to what is expected for a critical state, and consistent with either geometrical[12–14] or surface barriers[13,15] determining the hysteretic response. Figure 1(b) shows field profiles corresponding to the magnetization data presented in Fig. 1(a). A large gradient in the local field between the outer (sensors 2 and 11) and inner (sensors 3 and 10) edges of the crystal in increasing field (open symbols) implies that large screening currents flow on the edge of the sample. In the absence of significant bulk pinning vortices penetrating the geometrical or surface barrier are accelerated by the nonuniform demagnetizing field, forming a ''flux pool'' at the sample center and almost flux-free regions close to the sample edges. The domelike field profile observed in increasing applied field is one of the hallmarks of negligible bulk pinning and strong geometrical effects.[12–14] Slight asymmetry in the dome profiles is due to

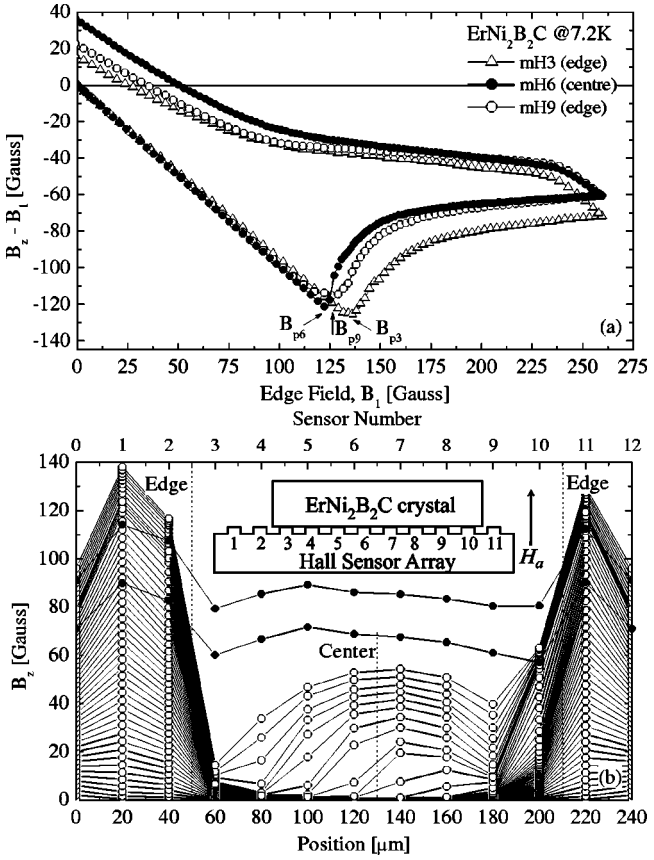

FIG. 1. (a) Local magnetization, $B_z - B_1$ vs B_1 at 7.2 K. (b) Field profiles measured for increasing (open symbols) and decreasing (closed symbols) field. Sensor positions 0 and 12 represent the external applied field. The inset to (b) shows the relative positioning of the crystal and Hall sensor array.

a locally weaker (stronger) surface and geometrical barrier on the right (left) hand crystal edge, shifting the minimum in free energy for a vortex in the almost pin-free crystal. In decreasing field (solid symbols) the observed profile is almost flat, or weakly domed across the sample. This means that vortices exit freely as the field is reduced and is consistent with negligible bulk pinning and the dominance of geometrical or surface barrier effects.

Figure 2 shows similar data to Fig. 1 at 2.75 K, well below the magnetic ordering transition, T_a^m. The magnetization loops in Fig. 2(a) are now increased in magnitude as expected at lower temperatures. Hysteresis is widest for the magnetization recorded at the sample center (sensor 6) with a much smaller magnetization recorded at the sample edges (sensors 3 and 9). This indicates that geometrical or surface barriers no longer dominate the vortex behavior at this temperature and that bulk pinning has become significant. A comparison of the penetration fields determined at the sample edges and center reveals complicated field penetration behavior as shown by the detailed increasing field profiles in Figs. 2(b) and 2(c) (sample temperature 2.5 K) (open symbols). Nonuniformities in the penetrating field profile are apparent in Fig. 2(b). Flux penetrates first at the right-hand edge forming an off-center ''bubble'' of flux at the right-hand side of the crystal. The presence of bulk pinning means

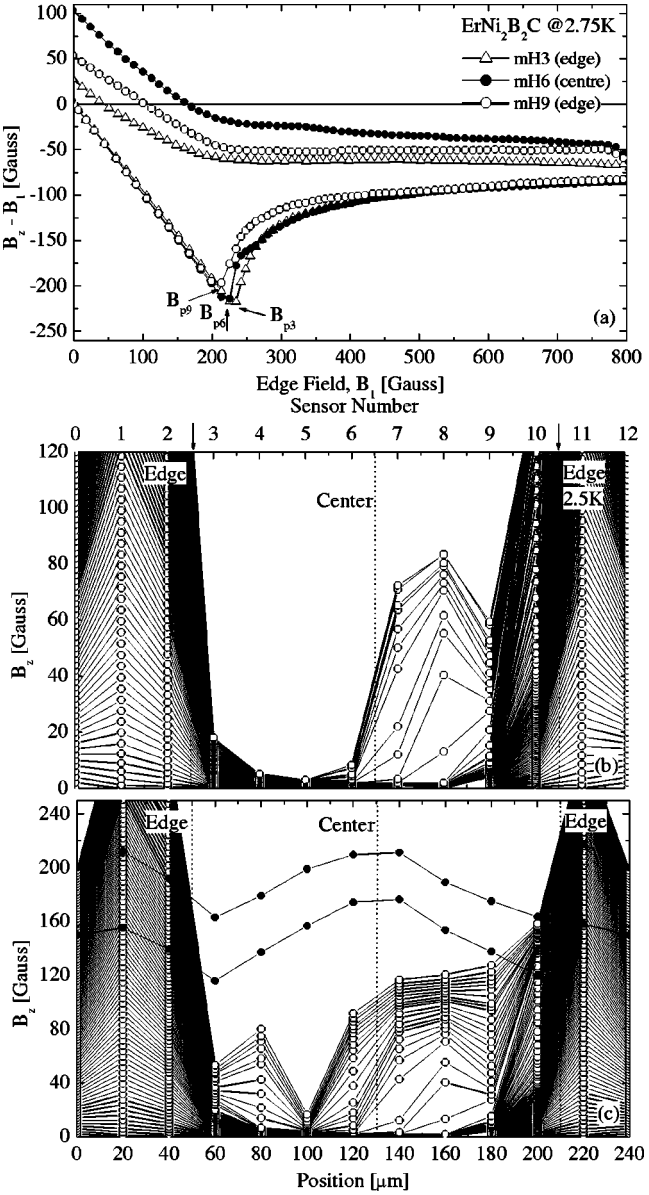

FIG. 2. (a) Local magnetization, $B_z - B_1$ vs B_1 at 2.75 K. (b) Detailed field profiles (2.5 K) showing the first penetration of vortices at the right-hand edge of the crystal followed by penetration of the left-hand edge at higher fields (c).

vortices are now prevented from spreading freely throughout the crystal, in contrast to the almost pin-free situation at higher temperatures [Fig. 1(b)]. Comparison of the data presented in Figs. 1 and 2 shows that weak asymmetry in the ascending field profile at high temperatures is ''amplified'' considerably by the onset of significant bulk pinning. A pinning determined critical state separates the flux-filled bubble from the flux-free central region,[12,14] as indicated by the steep field gradient at the left-hand side of the bubble. Only at much higher fields does flux penetrate the left-hand edge forming a second smaller flux bubble [Fig. 2(c)]. The ''double-dome'' flux profile shown in Fig. 2(c) is consistent with the field profiles predicted for a combination of weak bulk pinning operating together with the geometrical barrier.[12,14] Similar penetration of bubblelike domains of

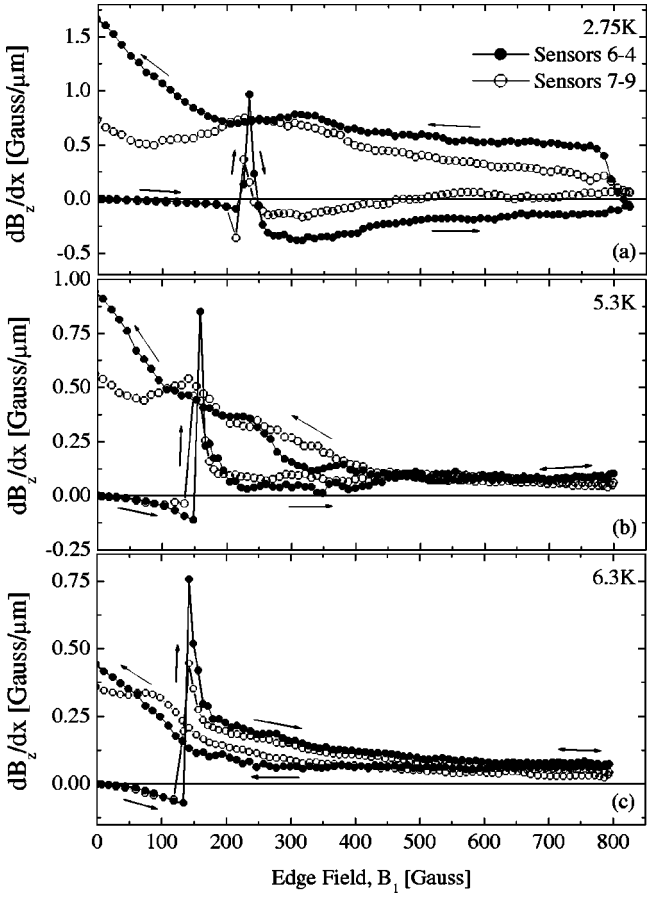

FIG. 3. Field gradient, dB_z/dx vs B_1 determined by sensors 6–4 (solid symbols) and 7–9 (open symbols) at temperatures of (a) 2.75 K, (b) 5.3 K, and (c) 6.3 K. ''Anticlockwise'' direction of the gradient loops in (a) and (b) is due to bulk pinning dominated behavior. The ''clockwise'' gradient loop in (c) is due to geometrical or surface barriers.

vortices has been observed by decoration measurements of $NbSe_2$ (Ref. 16) and recently by magneto-optical investigations of our $ErNi_2B_2C$ crystals.[17] We have measured three different crystals each with slightly differently prepared edges. These were either natural crystal edges, wire saw cut edges or cut edges polished until optically smooth with diamond impregnated polishing paper. The results obtained for each of the crystals confirmed to be common with differences in edge preparation found not to significantly effect the asymmetry of the initial penetrating field profiles. Since initial penetration of vortices occurs at the weakest edge defect and/or where the demagnetization field is highest it might be expected that asymmetric penetration of flux is the usual case when the surface or geometrical barrier operates together with bulk pinning effects.[16,17] Profiles obtained in descending applied field (solid symbols) are inverted and more symmetric compared to those in increasing field confirming the dominance of bulk pinning rather than competition with an asymmetric surface or geometrical barrier.

Analysis of the field gradient dB_z/dx allows us to differentiate more precisely between surface and bulk current flow, as described in Refs. 11 and 13. Here we approximate

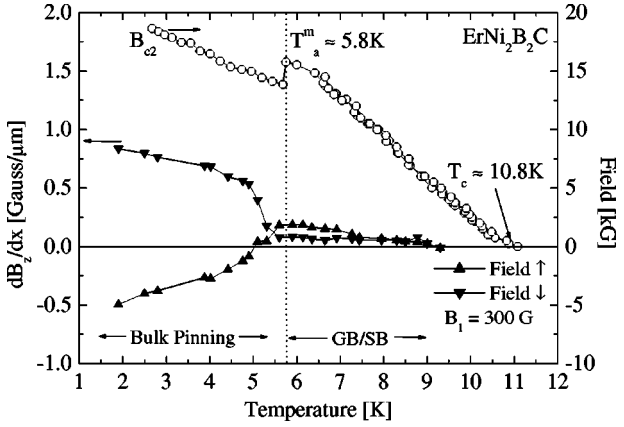

FIG. 4. (Left axis) dB_z/dx vs temperature for increasing (up triangle) and decreasing (down triangle) field cycles at $B_1 = 300$ G. Bulk pinning ''switches on'' below about 5.5 K, close to the onset of an *a*-axis incommensurate magnetic ordering of the Er moments at T_a^m (dashed line). (Right axis) B_{c2} as determined by resistivity and *global* magnetization (open circles).

dB_z/dx as the difference between the local field measured at the sample center-left (sensor 6) and left-hand side (sensor 4) divided by their spatial separation (40 μm). We also make a second determination of dB_z/dx using the center-right (sensor 7) and right-hand side (sensor 9). This is illustrated in Fig. 3 for data collected at temperatures of (a) 2.75 K, (b) 5.3 K (just below T_a^m), and (c) 6.3 K (just above T_a^m). Determination of the internal field gradients from both pairs of sensors provides a useful consistency check of the analysis presented below in view of the strong asymmetry in the penetration field behavior close to B_p. In Figs. 3(a) and 3(b) dB_z/dx traces out ''anticlockwise'' loops consistent with bulk pinning controlling the hysteretic response. Asymmetry in the magnitude of dB_z/dx between the ascending and descending branches of the loop indicates that even at low temperatures, when bulk pinning is significant, the geometrical barrier continues to modify the profiles in ascending field [Fig. 2]. Since the geometrical barrier does not significantly affect the profiles in decreasing field, an estimate for the critical current density can be made from dB_z/dx in this case and is of the order $10^4 \mathrm{Acm}^{-2}$ at 2.75 K. The gradient loops in Fig. 3(c) show quite different behavior to Fig. 3(a), where dB_z/dx is always positive and traces out ''clockwise'' hysteresis loops, consistent with the geometrical barrier dominating the hysteretic response.

In Fig. 4 we use the above analysis of the field gradients to identify more precisely the temperature regimes in which bulk pinning and geometrical or surface barriers dominate the hysteretic vortex response. Figure 4 (left axis) presents dB_z/dx (sensors 6–4) obtained from magnetization loops at various temperatures at the same value of the edge field, $B_1 = 300$ G (greater than B_p for the temperature range investigated). dB_z/dx should be negative (positive) in increasing (decreasing) field and of similar magnitude for increasing and decreasing branches of the hysteresis loop when bulk pinning effects dominate the vortex behavior [Fig. 3(a)]. In the case of geometrical or surface barriers being dominant dB_z/dx should be positive in increasing field and close to

zero in decreasing field [Fig. 3(c)]. A crossover between these two behaviors is clear in Fig. 4 at a temperature of about 5.5 K. The magnetic ordering temperature, T_a^m, and upper critical field, B_{c2} are also shown in Fig. 4 (right axis) as determined by global magnetization and resistivity measurements on crystals from the same batch. The coincidence between the onset of bulk pinning and magnetic order at T_a^m is remarkable.

The data presented here for $ErNi_2B_2C$ and in Ref. 11 for $HoNi_2B_2C$ indicate a strong correlation between the onset of significant pinning effects and the appearance of the *a*-axis incommensurate magnetic ordered phase. Figure 4 shows that B_{c2} is suppressed below T_a^m consistent with the notion of pair breaking in the magnetically ordered state.[4,5,10,18] Changes in the superconducting parameters below T_a^m are likely to also lead to changes in the vortex properties.[10] It might not be surprising therefore, that pair breaking below this temperature should also modify flux pinning. $HoNi_2B_2C$ also exhibits strong pair breaking upon ordering into the *a*-axis incommensurate phase between $T_{AF}^m \simeq 5$ K$< T < T_a^m \simeq 6$ K resulting in a deep minimum in B_{c2} close to T_{AF}^m.[4,5] Below T_{AF}^m, B_{c2} recovers with decreasing temperature in the commensurate AF phase but never regains a value close to that expected from extrapolation of the higher temperature part of the curve in the nonmagnetic state. This suggests that pair breaking weakens but does not disappear upon entering the commensurate AF state at T_{AF}^m in agreement with theoretical analysis.[18] We only observe significant pinning effects between about 5 and 6 K for $HoNi_2B_2C$ coincident *exclusively* with the existence of the *a*-axis incommensurate spiral[11] and not associated with the incommensurate *c*-axis modulation or the commensurate AF order above and below this temperature range, respectively. This suggests that pair breaking due to onset of magnetic order alone cannot entirely account for the enhanced vortex pinning observed here for $ErNi_2B_2C$ and in Ref. 11 for $HoNi_2B_2C$.

Recently, Gammel *et al.*[19] have reported pinning studies of $ErNi_2B_2C$ in the weak ferromagnetic phase using transport and global magnetization techniques. At low temperatures bulk pinning is enhanced by almost a factor of three upon entering the weak ferromagnetic phase below $\simeq 2.5$ K. They propose that the ferromagnetic component, associated with a ''squaring up'' of the *a*-axis modulation,[3] leads to ''sharp'' ferromagnetic domain boundaries which may cause additional pair breaking and therefore enhanced pinning at the domain walls. An extrapolation of their critical current density measured above 2.5 K indicates that J_c becomes small for temperatures approaching T_a^m, consistent with the results presented here, although they are unable to separate contributions from bulk and surface current flow. High resolution x-ray[20] diffraction studies show that the crystal lattice becomes orthorhombic with increasing distortion ($\simeq 0.2\%$) for temperatures below T_a^m leading to the possibility of structural, as well as magnetic domains. Since the vortex lattice is already coupled to the crystal lattice, as indicated by its preferred orientation, the appearance of structural domains may also present pinning effects for vortices.[17] These scenarios are consistent with our observations of enhanced pinning coinciding with the occurrence of the *a*-axis modulated magnetic structure in $ErNi_2B_2C$ [and $HoNi_2B_2C$ (Ref. 11)] and combined weak ferromagnetic component below $\simeq 2.5$ K in Ref. 19.

In summary, we have used a miniature local Hall array to investigate vortex pinning in single crystals of the magnetic superconductor $ErNi_2B_2C$. Geometrical and surface barriers dominate the vortex behavior over a large part of the low-field magnetic phase diagram. Bulk pinning only becomes important below about 5.5 K coinciding with the appearance of the *a*-axis incommensurate magnetic spiral state. We propose that particular components of the magnetic order in both $ErNi_2B_2C$ (and $HoNi_2B_2C$), or domains thereof, interact directly with the vortex lattice leading to a pinning of vortices.

E.Z. acknowledges support by the German-Israel Foundation G.I.F.

*Present address: Institute Laue Langevin, BP156-38042, Grenoble, France. Email address: dewhurst@ill.fr

†Present address: Scientific Generics, Harston Mill, Cambridge CB2 5NH, UK.

[1] J. W. Lynn *et al.*, Phys. Rev. B **55**, 6584 (1997).
[2] P. C. Canfield *et al.*, Phys. Today **51**, 40 (1998).
[3] S. K. Sinha *et al.*, Phys. Rev. B **51**, 681 (1995).
[4] A. I. Goldman *et al.*, Phys. Rev. B **50**, 9668 (1994).
[5] A. Kreyssig *et al.*, Physica B **234-236**, 737 (1997).
[6] H. Kawano *et al.*, J. Phys. Chem. Solids **60**, 1053 (1999).
[7] U. Yaron *et al.*, Nature (London) **382**, 236 (1996).
[8] M. R. Eskildsen *et al.*, Phys. Rev. Lett. **78**, 1968 (1997).
[9] D. McK. Paul *et al.*, Phys. Rev. Lett. **80**, 1517 (1998).
[10] P. L. Gammel *et al.*, Phys. Rev. Lett. **82**, 1756 (1999).
[11] C. D. Dewhurst *et al.*, Phys. Rev. Lett. **82**, 827 (1999).
[12] E. Zeldov *et al.*, Phys. Rev. Lett. **73**, 1428 (1994).
[13] E. Zeldov *et al.*, Europhys. Lett. **30**, 367 (1995).
[14] E. H. Brandt, Phys. Rev. B **59**, 3369 (1999).
[15] C. P. Bean and D. J. Livingston, Phys. Rev. Lett. **12**, 14 (1964).
[16] M. Marchevsky *et al.*, Phys. Rev. Lett. **75**, 2400 (1995).
[17] N. Saha *et al.*, Phys. Rev. B **63**, 020502(R) (2001).
[18] A. Amici *et al.*, Phys. Rev. Lett. **84**, 1800 (2000).
[19] P. L. Gammel *et al.*, Phys. Rev. Lett. **84**, 2497 (2000).
[20] C. Detlefs *et al.*, Phys. Rev. B **56**, 7843 (1997).